

Power Spectral Analysis of Enhanced Scintillation of Quasar 3C459 due to Comet Halley

P. Janardhan,^A S. K. Alurkar,^A A. D. Bobra,^A O. B. Slee^B and D. Waldron^C

^A Physical Research Laboratory, Navrangpura. Ahmedabad 380 009, India.

^B Australia Telescope National Facility, CSIRO, P.O. Box 76, Epping, N.S.W. 2121, Australia.

^C UK Schmidt Telescope Unit, Royal Observatory, Edinburgh.

Abstract

The radio source 2314+038 (3C459) showed enhanced scintillations on three days at a solar elongation of about 90° as the plasma tail of Halley's Comet swept across it on six days during 16–21 December 1985. If we assume that the plasma velocities in the tail were not constant everywhere, but increased linearly from about 50 km s^{-1} at the tail axis to the normal average solar wind velocity of 400 km s^{-1} at the edges where the tail merged with the solar wind, a power spectral analysis of the scintillations shows two ranges of the rms electron density variation ΔN and scale size a . In particular, these are a fine scale zone near the axis where a is in the range 9 to 27 km and ΔN in the range 2 to 5 cm^{-3} and a zone near the edges with a and ΔN in the ranges 100 to 265 km and 0.4 to 0.8 cm^{-3} respectively. The assumption of a single velocity of 100 km s^{-1} throughout the tail shows similar fine scales near the tail axis and large scales near the edges. The scale sizes in that case range from about 18 km at the axis to about 70 km at the edges, corresponding to ΔN of 3.3 and 0.85 cm^{-3} respectively. A comparison with the results obtained by Slee *et al.* (1987) shows that there is no radial variation of ΔN . The tail-lag is seen to play a crucial role in determining the correct occulting geometry and the path of the source through the tail.

1. Introduction

The recent observations of Comet Wilson (Slee *et al.* 1990) during its occultation of two quasars in May 1987 have shown the presence of two scintillating regimes in the plasma tail, one a small-scale turbulence of 10 to 40 km close to the axis and a second large-scale turbulence of 90 to 350 km in the transition region where the tail merges with the solar wind. A second look at the observations by Alurkar *et al.* (1986) was thus undertaken to see if a similar trend, if any, could be observed in the tail of Halley's Comet. Also, the interaction of the radially directed solar wind with the comet's velocity causes the tail to deviate from the true radial direction by a few degrees. This tail-lag, which can be as much as 5° (Belton and Brandt 1966), is crucial in determining the correct occulting geometry and it was not allowed for in the observations of Alurkar *et al.* (1986). The analysis has also provided an opportunity to recalculate more accurately and with better calibration the scintillation indices reported in the earlier paper.

These values were overestimated as no allowance was made for the effect of automatic gain control in the receiving system during the 103 MHz observations in December 1985.

Recent high resolution H_2O^+ emission spectra (Scherb *et al.* 1990) have been used to measure the Doppler shifts of emission lines and to determine directly the outflow velocities of the plasma in the coma and tail. These measurements yield an average velocity of H_2O^+ ions on 16 December 1985 of about 45 km s^{-1} up to $2 \times 10^6 \text{ km}$ from the nucleus. Photographic studies of the displacement of features in cometary plasma tails have been used to infer velocities in the range 20 to 250 km s^{-1} (Celnik and Schmidt-Kaler 1987; Jockers 1981, 1985). Several theoretical studies of the morphology and formation of ion tail structures have also been conducted (Ip *et al.* 1982, 1985; Miller 1970; Schmidt and Wegmann 1982). In the case of structures like rays—plasma sheets sandwiched between regions of opposite magnetic polarity—it has been found (Ness and Donn 1965) that tail-aligned flow speeds in these structures must vary linearly across a width of $(1-2) \times 10^5 \text{ km}$. A photographic study (Saito *et al.* 1987) has shown the presence of rays in Comet Halley's tail from mid December 1985 to January 1986. In more recent work Schmidt-Voigt (1989) carried out a three-dimensional time-dependent MHD model of cometary plasmas and showed that condensations move down the tail with a velocity of 20 to 70 km s^{-1} .

The occulting geometry during the present observations was such that accurate estimates of the rms electron density variation ΔN and scale size a could be obtained on each day during 16–21 December 1985 at different distances with respect to the tail axis and nucleus, provided an estimate of the velocity of the plasma at that point in the tail was made. These observations were made between $(6-30) \times 10^6 \text{ km}$ downstream of the nucleus where no accurate estimates or observations of ion velocities are available. The simplest assumption therefore would be that of a single velocity of about 50 or 100 km s^{-1} at all points across the width of the tail. Such an assumption, though, would be unrealistic because one expects that at the interaction zone where the tail merges with the solar wind, the velocity must be equal to that of the undisturbed solar wind. In the following analysis therefore it is assumed that the velocity varies linearly across the tail having a value of 50 km s^{-1} at the tail axis and attaining 385 km s^{-1} at the edge of the tail. This is based on the velocity measurements of H_2O^+ ions in the tail of Halley's Comet (Celnik and Schmidt-Kaler 1987) which give velocities of about 50 to 140 km s^{-1} in the range 6 to $30 \times 10^6 \text{ km}$ downstream of the nucleus. The value of 385 km s^{-1} was the average solar wind velocity in the direction of the source 3C459 between 17 and 21 December 1985, as measured at the three station IPS network in Japan operating at 327 MHz. The distance of the occulted source (3C459) with respect to the tail axis on each day was calculated using the wind-sock model (Hajivassiliou and Duffett-Smith 1987), with an opening angle of 7° as measured on a masked and contrast-enhanced UK Schmidt photograph of the comet and a coma radius of 10^{-3} AU .

Enhanced scintillations were also observed at 103 MHz when the tail of Comet Austin occulted the radio source 2204+29 on 13 May 1990 (Janardhan *et al.* 1991). This analysis assumed a tail-lag of $+3^\circ$ for the tail and also showed a fine scale and high ΔN zone close to the axis of the comet tail. Although the occultation took place on one day only, the results obtained provided further

reason to reanalyse the data obtained from Halley after taking into account the effects of the tail-lag.

2. Observations and Analysis

The observations were carried out with the 10,000 m² dipole antenna array at Thaltej, near Ahmedabad, India. This antenna is a filled aperture phased array made up of 2048 full-wave dipoles. The array is divided into two halves, namely the north and south. Each half comprises 32 transmission lines loaded with 32 dipoles, polarised horizontally in the N-S direction to form a correlation-type interferometer observing sources at meridian transit. Thirty-two beams are formed by each half of the array using a beam-forming network called the Butler matrix, which is essentially the analogue equivalent of a fast Fourier transform. These beams are deployed in declination and are each 1.8° N-S × 3.6° E-W and cover ±30° of declination centred on the zenith. A pair of identical beams is connected during each observation to a correlation-type receiver which yields sine and cosine quadrature outputs. The rapidly changing intensity fluctuations are picked up by a device called the scintillometer with an output proportional to the square of the scintillating flux of the source. A full description of the system can be found in the paper by Alurkar *et al.* (1989).

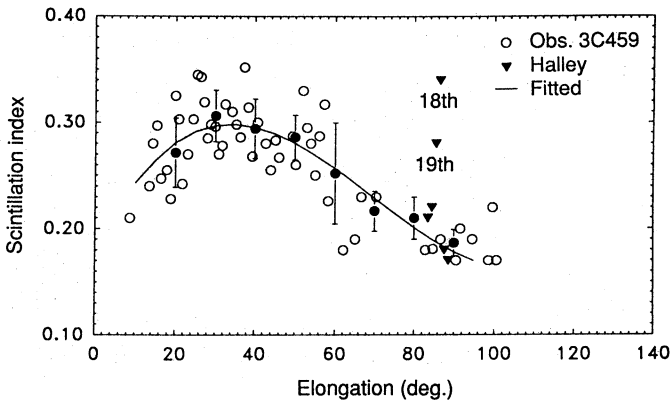


Fig. 1. Variation of the scintillation index m as a function of solar elongation for the occulted source 3C459, shown by open circles. The triangles represent the scintillation index measured between 16 and 21 December, while the solid circles represent the mean value in each 10° bin. The curve is a third-order polynomial fit to the data. Note the small scatter at 90° compared with the enhancement in scintillation on 18 and 19 December.

The occulted source was regularly observed between mid-1984 and the end of 1987. Fig. 1 shows a plot of the variation of the scintillating index (rms flux/mean source flux) with solar elongation ϵ for all data obtained in this period. The open circles represent the scintillation indices which have been averaged into one-degree bins and then fitted by a third-order polynomial. This matches well with the values expected from the RKH model (Readhead *et al.* 1978). The triangles represent the scintillation indices obtained during 16–21 December 1985, when the tail of Halley occulted the source. These values have not been considered

when making the fit. A standard error bar is shown for each 10° bin, with the solid circles showing the mean value in each bin. It can be seen that there is an enhancement by a factor of about 2 in m compared with the expected value of about 0.19 from the third-order fit and about 0.18 as calculated from the RKH model. From Fig. 1 it is apparent that this enhancement is very significant when compared with the scatter at a solar elongation of 90° . All indices m were obtained from the measured deflections on a strip chart of the sine, cosine and scintillometer outputs, after correcting the deflections of the sine and cosine channels for the effects of automatic gain control. The calibration procedure was that suggested by Duffett-Smith (1986). Table 1 gives the scintillation indices and other important parameters calculated for 3C459 during the occultation between 16 and 21 December.

Table 1. Parameters for the source 2314+038 (3C359)

The source has a gaussian diameter of 0.41 arcsec (estimated from 103 MHz observations using the RKH model) and a mean source flux of 43 Jy (Readhead and Hewish 1974)

Date	Transit (UT)	Elongation (deg.)	Dist. from nucleus (AU)	Dist. from axis (10^5 km)	Scintillation index
16-12-85	1246	88.6	0.04	5.17	0.17 ± 0.015
17-12-85	1242	87.6	0.08	2.59	0.18 ± 0.015
18-12-85	1238	86.5	0.12	0.00	0.34 ± 0.015
19-12-85	1234	85.5	0.14	1.29	0.28 ± 0.015
20-12-85	1230	84.5	0.18	3.88	0.22 ± 0.015
21-12-85	1226	83.5	0.20	5.17	0.21 ± 0.015

On 18 December when the observed scintillating power was at a maximum, the position angle (PSANG) of the comet tail was 65.9° . To bring out the crucial nature of the tail-lag, the tail axis has been plotted in Fig. 2 at 10 hours UT on 18 December, and 0 and 10 hours UT on 19 December for three different values of tail-lag, i.e. $65.9^\circ - 3^\circ$, 65.9° and $65.9^\circ + 3^\circ$. It can be seen that for the case when the tail-lag is -3° the source was closest to the axis on 18 December during the transit at 1238 UT. On the other hand, for a tail-lag of 0° the tail axis would not have passed across the source until 22 December while for a tail-lag of $+3^\circ$ the date of passage of the axis across the source would have been much before 18 December. The tail-lag is thus a crucial factor in deciding the actual time of passage of the source across the tail axis and the correct path of the source through the tail. Fig. 3 shows the actual path of the source 3C459 through the comet tail for a tail-lag of -3° . It can be seen that the source cut across the tail moving progressively downstream of the nucleus, being on the edge of the tail on 16 December at a distance of 0.04 AU from the nucleus (measured along the axis), on the axis and 0.12 AU downstream on the 18th and on the other edge and 0.2 AU downstream on the 21st.

The position angle of the tail axis was also measured from a contrast-enhanced photographic plate taken with the UK Schmidt telescope. The original plate was a 40 minute exposure on IIIaJ emulsion with a UG 395 filter (395–540 nm), with the midpoint of exposure at 10h 14m 30s UT, 13 December 1985. The original plate (J10591T) was copied using a high contrast unsharp-masking technique, whereby the original was exposed in a diffuse-light contact copy unit, on to continuous-tone film. A 2 mm thick sheet of glass was used to separate the

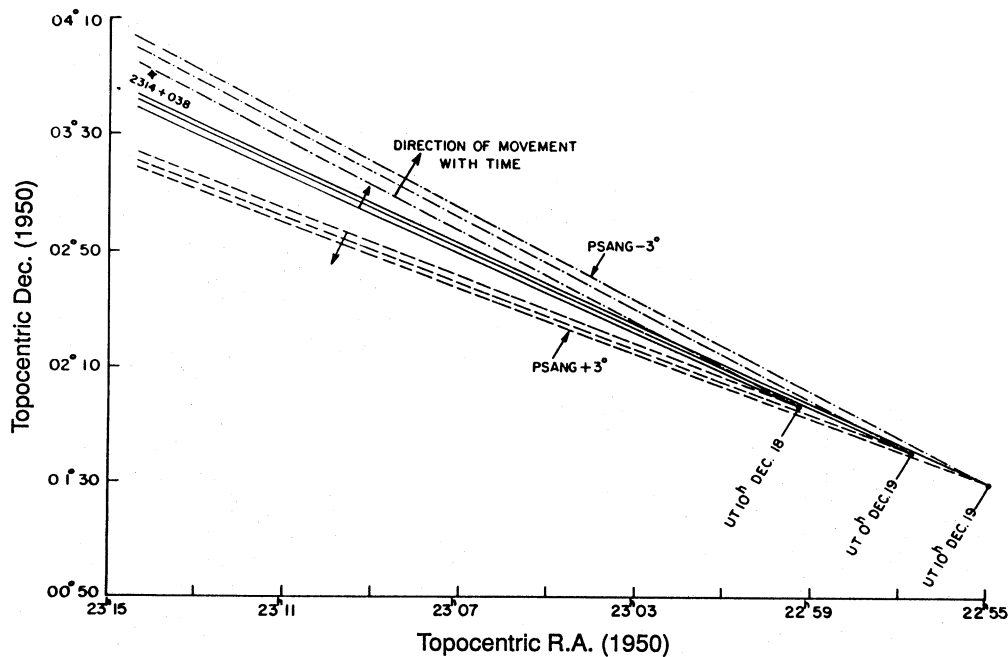


Fig. 2. Tail axis of the comet is shown for varying values of tail-lag correction, i.e. $65.9^\circ + 3^\circ$, 65.9° and $65.9^\circ - 3^\circ$. For each of these values of position angle (PSANG) the axis has been drawn at the three different values of UT indicated.

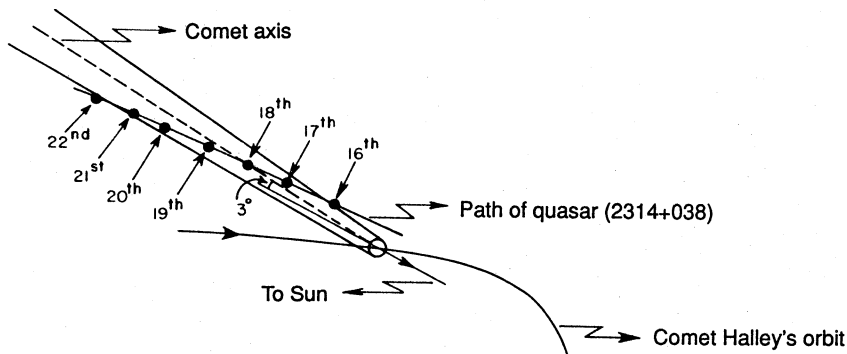


Fig. 3. Actual path of the source 3C459 through the tail of the comet plotted for tail-lag correction of -3° (not to scale).

original and the film, so that an unsharp positive copy was obtained. This was exposed and processed to appropriate density and contrast, and once dry was fixed to the glass side of the original plate. The effect of this was to mask the general large-scale density variations, leaving the fine detail unaffected. A contact copy of the masked original was then made using high contrast line film. The result was a film positive which was used to create a paper print in the normal manner.

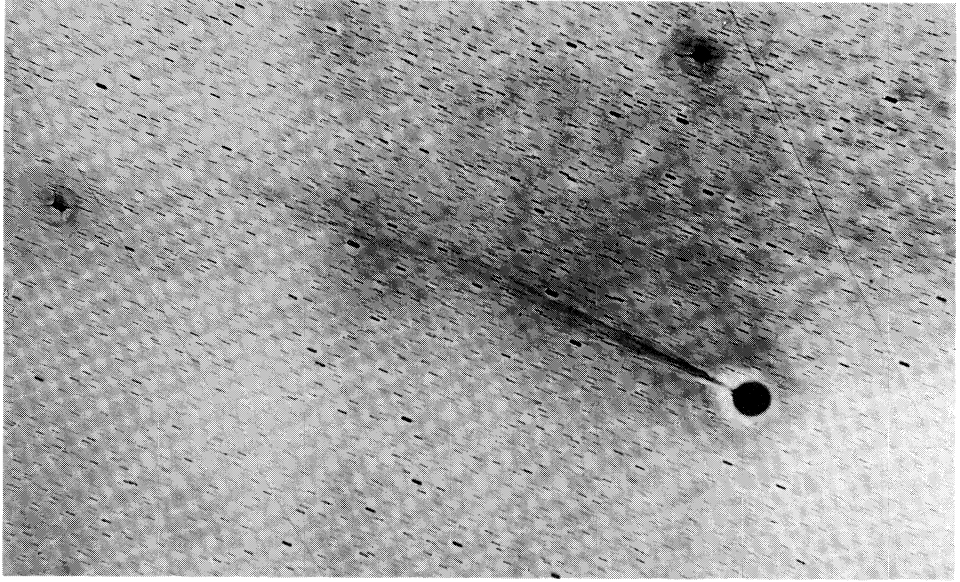


Fig. 4. Masked and contrast-enhanced UK Schmidt photograph of Comet Halley. The original plate was a 40 minute exposure with a UG 395 filter (395–540 nm). The midpoint of exposure was at 10h 14m 30s UT, 13 December 1985.

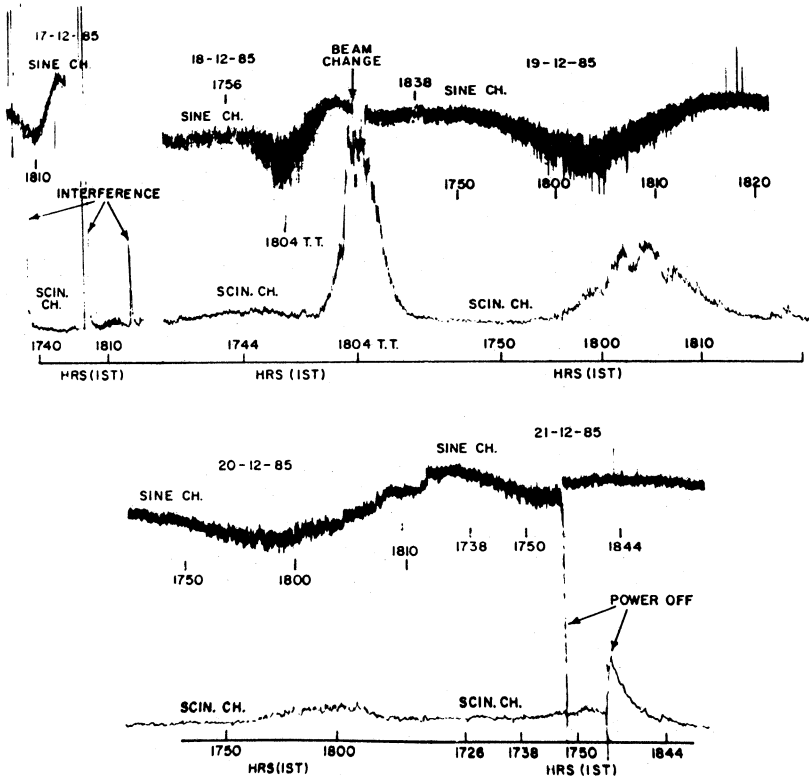


Fig. 5. Actual three-channel chart recorder output of the observation. The two traces shown are the sine and scintillometer outputs.

The cone of plasma emission extending out to about 30 arcmin is well defined and is seen to converge sharply onto the nucleus, as shown in Fig. 4, which is a copy of the actual contrast-enhanced UK Schmidt plate obtained by the above procedure. This cone of plasma is seen to cover a range of position angles from 60.6° to 67.6° . Taking the average of these two values, i.e. 64.1° , to define the tail axis and comparing it with the anti-solar position angle of 67° on the evening of 13 December 1985, we obtain a value of the position angle correction of $-2.9^\circ \pm 0.5^\circ$. On this print the tail can also be traced out to about 4.0° , where the plasma is seen to be contained within a transverse angular size of about 7.0° , corresponding to a linear size of approximately 1.7×10^6 km.

Fig. 5 shows the actual chart recordings of the source 3C459 between 16 and 21 December. The two traces shown on each day are the sine and scintillometer outputs of the correlation receiver. Fig. 6 shows the power spectra obtained for each day between 16 and 21 December. The power spectra were computed by subtracting a Hanned spectrum of 10 minutes of data off-source, from a Hanned spectrum of 10 minutes of data on-source. The on-source data were taken for 5 minutes on either side of the transit time on each day from the available on-source data of about 15 minutes. The data were sampled at 20 Hz, digitised using a 12 bit, ± 5 V A/D converter (Alurkar *et al.* 1989) and stored on magnetic tape for analysis. On 21 December, however, due to a power failure (see Fig. 5) during transit of the source through the beam, only ± 2 minutes of data were available on-source. The spectrum was thus obtained by subtracting a Hanned spectrum of 10 minutes off-source data from a Hanned spectrum of 4 minutes on-source data. All spectra were normalised to the highest spectral density and had a frequency resolution before Hanning of 0.0813 Hz. It can be seen that the spectrum of 18 December has a peak around 0.33 Hz which slowly decayed out to about 3.5 Hz; this is a very typical IPS spectrum. On the 16th, when the source was at the edge of the tail, the spectrum decayed much faster than on the 18th, with the peak being around 0.16 Hz. The decay on the 17th is seen to be slower, though the peak does not shift. On the 19th the source was still close to the axis and the spectrum showed a less rapid decay than on 16th and 17th and went out to about 2.5 Hz, with the peak at about 0.24 Hz. On the 20th the decay was a little faster than on the 19th and went out to about 1.5 Hz. The spectrum of the 21st had much more noise, compared with other days, but clearly had some scintillating power.

It is important to note the clear shift in the peak from 0.16 Hz on the 16th to 0.33 Hz on the 18th when the source was closest to the axis, and to 0.24 Hz

Table 2. Spectral width and rms phase deviation

Date	f_2 (Hz)	ϕ (rad)
16-12-85	0.23	0.12
17-12-85	0.31	0.13
18-12-85	0.87	0.24
19-12-85	0.56	0.20
20-12-85	0.34	0.16
21-12-85	0.49	0.15

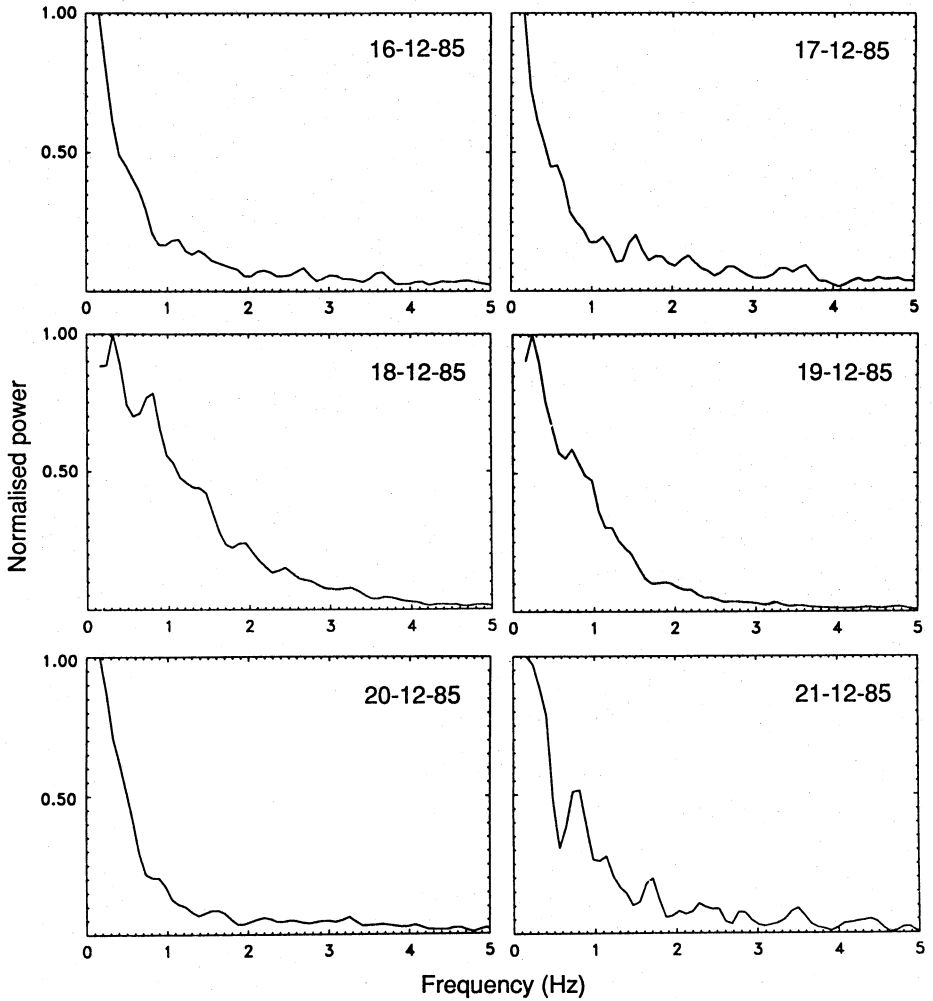


Fig. 6. Power spectra obtained on each day between 16 and 21 December. The spectra have been normalised to the highest spectral density and have a frequency resolution before Hanning of 0.0813 Hz. Note the clear shift in the peak of the spectrum to higher frequencies on the 18th and 19th.

Table 3. Scale size and rms electron density deviation for varying velocities

Date	Dist. from axis ^A ($\times 10^5$ km)	Velocity ^B (km s^{-1})	a (km)	ΔN (cm^{-3})
16-12-85	5.17	385.00	266	0.43
17-12-85	2.59	192.54	99	0.77
18-12-85	0.00	50.00	9	4.68
19-12-85	1.29	96.23	27	2.26
20-12-85	3.88	288.77	135	0.81
21-12-85	5.17	385.00	125	0.79

^A Calculation uses a correction of -3° for the tail-lag.

^B Obtained by assuming a linear gradient in velocity as one moves from the tail axis to the edge.

on the 19th. If the shift in the peak to higher frequencies were not present, then it would have meant that other processes like ionospheric scintillation or gain changes were responsible for obscuring the true peak due to the plasma in the tail. Table 2 gives the spectral widths measured on each day from the power spectrum and the rms phase deviation imposed on the wave emerging from the screen.

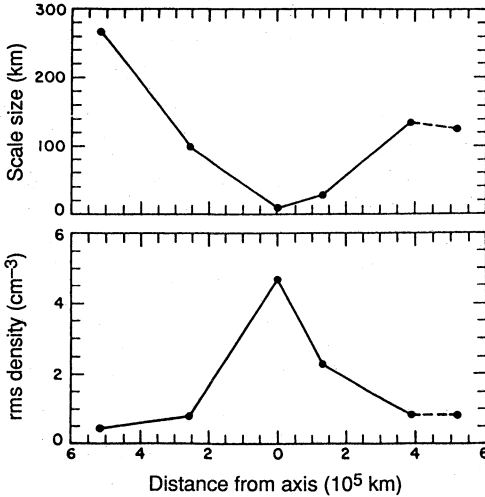


Fig. 7. Variation of scale size a and rms electron density ΔN as a function of distance away from either side of the tail axis.

If we assume that the thin screen theory developed by Salpeter (1967) is valid for these observations, the correlation length or scale size is given by

$$a = \frac{V}{2\pi f_2},$$

where V is the velocity of the diffraction pattern across the observer and f_2 the width of the power spectrum at the $\exp(-0.5)$ points. For a circularly symmetric gaussian electron density correlation function, the rms phase deviation imposed across the wave emerging from the screen is given by (Little 1976)

$$\phi = (2\pi)^{1/4} (\lambda r_e) (aL)^{1/2} \Delta N,$$

where the classical electron radius r_e is equal to 2.82×10^{-13} cm, λ is the operating wavelength of 291 cm, ΔN the rms electron density and L the thickness of the screen, here taken to be 1.7×10^6 km. This value is obtained by assuming that the thickness of the tail is equal to the width measured on the contrast-enhanced UK Schmidt photograph of 13 December. Also, for weak scattering the scintillation index is given by $m = \sqrt{2} \phi$.

If one assumes that the velocity of the plasma in the tail varies as described earlier, from a value of 50 km s^{-1} at the axis to 385 km s^{-1} at the edge, then a and ΔN of the turbulence can be calculated using the above equations. Table 3 summarises these values while Fig. 7 plots the variation of a and ΔN as a

function of distance away from the axis. It can be seen that on and near the axis (during the 18th and 19th) a is in the range 9–27 km which is much finer than expected in normal IPS from the solar wind. On the 16th and 17th a is in the range 100 to 266 km which is a normal IPS scale size. Again on the 20th, when the position of the source with respect to the tail axis was neither at the edge nor on the axis, a scale size of 135 km is obtained with ΔN between 2.3 and 4.7 cm^{-3} near the axis and between 0.4 and 0.8 cm^{-3} near the edge. Since the spectrum on the 21st has been derived from very few blocks of data near transit, these points have been marked by a dashed line in Fig. 7.

3. Results and Discussions

A comparison of our results with those for Comet Wilson is instructive. Slee *et al.* (1990) derived a fine scale turbulence between 10 and 40 km for a range of velocities between 100 and 400 km s^{-1} , while the present results—which are statistically more significant due to the larger number of observations across the tail—suggest that the actual scale size is a more sensitive function of the velocity than was seen earlier. One can now say that a fine regime of scale sizes dominated by high values of ΔN exists along and close to the axis of cometary plasma tails. The ΔN in this region is about an order of magnitude greater than that expected in the normal solar wind at heliocentric distances of about 1 AU (Cohen *et al.* 1967). A larger scale size regime along and close to the edge is also seen to exist, but the range could be from 100 to 265 km. This region is dominated by a value of ΔN which is much closer to the normal solar wind value. The analysis also suggests that the physical processes at work close to the axis of the comet are independent of the solar wind and hence show different characteristics, whereas as one moves towards the edges of the plasma tail, the solar wind effects begin to dominate and slowly damp out the effects of the processes dominant at the axis. A detailed magnetohydrodynamic model study will be required though before anything definite can be said about the actual processes at work.

The post-perihelion observations (Slee *et al.* 1987) of Comet Halley in March 1986 measured a ΔN of 1.9 cm^{-3} at a distance of 0.036 AU downstream of the nucleus. If one were to make allowance of about $+3^\circ$ in this case for the post-perihelion period, the point of occultation would have been near the edge and not along the axis of the comet. Also, the width of the tail measured from the masked and contrast-enhanced photo of the comet (Fig. 4) is greater than the value used by Slee *et al.* (1987) by a factor of about 3.5. If this difference in width is corrected for, the value of ΔN for the observations of Slee *et al.* (1987) would have to be reduced by a factor of $\sqrt{3.5}$, giving $\Delta N = 1 \text{ cm}^{-3}$. This value is thus identical to our $\Delta N = 1 \text{ cm}^{-3}$ which is the average for the data 16, 17, 19, 20 and 21 December when the source was not close to the axis of the tail. Thus it appears that provided the rate of ionisation of nuclear material remains unchanged over a period of a few months, there was no radial variation in ΔN in the off-axis region of the tail, though more observations would be required to confirm this. This is consistent with the model (Ip and Axford 1982) of ion composition for a Halley-type comet at a distance of 1 AU from the Sun. The model predicts negligible dependence of ion density on axial distance beyond 10^6 km downstream of the nucleus.

Table 4. Scale size and rms electron density deviation for a velocity of 100 km s^{-1}

Date	Dist. from axis ($\times 10^5 \text{ km}$)	a (km)	ΔN (cm^{-3})
16-12-85	5.17	69	0.85
17-12-85	2.59	51	1.07
18-12-85	0.00	18	3.31
19-12-85	1.29	28	2.22
20-12-85	3.88	47	1.38
21-12-85	5.17	33	1.55

Even if one were to assume a velocity of 100 km s^{-1} for the plasma throughout the tail, a fine scale turbulence zone is seen on and near the axis. The value of a lies between 18 and 28 km and ΔN between 2.2 and 3.3 cm^{-3} . The zone near the edge though is not so distinct with a and ΔN in the ranges 33 to 70 km and 0.9 to 1.6 cm^{-3} respectively. In conclusion, it can thus be said that evidence for the presence of fine scale turbulence dominated by high values of ΔN along and near the axis of cometary plasma tails is strong. Table 4 gives a and ΔN obtained for Halley by assuming a velocity of 100 km s^{-1} throughout the tail.

A similar study conducted during the occultation of the source 2204+29 by Comet Austin in May 1990 has also shown the presence of a fine scale region close to the axis, dominated by a similarly high value of ΔN and small a (Janardhan *et al.* 1991). In this analysis the tail-lag was assumed to be $+3^\circ$ and the a values obtained were in the range 17 to 68 km, while ΔN was in the range 3 to 6 cm^{-3} . The range in these values was due to the uncertainty in velocities by a factor of 4, from 100 to 400 km s^{-1} . The source, at the time of the occultation, was about 2° off the tail axis and 7.3° downstream of the nucleus. The occultation, though, took place on one day only. It can be seen that these values are comparable with those of Comet Halley during 18 and 19 December when the source was close to the axis.

Acknowledgments

We thank the staff of the Radio Astronomy group for their help and cooperation. In particular we are grateful for the meticulous observations made by Dr A. K. Sharma and Mr S. L. Kayasth. Our thanks are also due to Mrs Medha Alurkar for her help in programming. We would also like to thank Rekha Jain, University of St Andrews, Scotland, for her help. Financial assistance for this work came from the Departments of Space and Science & Technology, Govt of India and the Special Foreign Currency (SFC) project NA87AA-D-ER046 under Indo-US collaboration.

References

- Alurkar, S. K., Bhonsle, R. V., and Sharma, A. K. (1986). *Nature* **322**, 439.
 Alurkar, S. K., Bobra, A. D., Nirman, N. S., Venat, P., and Janardhan, P. (1989). *Ind. J. Pure Appl. Phys.* **27**, 322.
 Belton, M. J. S., and Brandt, J. C. (1966). *Astrophys. J. Suppl.* **13**, 125.
 Celnik, W. E., and Schmidt-Kaler, Th. (1987). *Astron. Astrophys.* **187**, 233.
 Cohen, M. H., Gundermann, E. J., Hardebeck, E. H., and Sharp, L. E. (1967). *Astrophys. J.* **147**, 449.

- Duffett-Smith, P. J. (1976). Ph.D. Thesis, Univ. of Cambridge.
- Hajivassiliou, C. A., and Duffett-Smith, P. J. (1987). *Mon. Not. R. Astron. Soc.* **229**, 485.
- Ip, W. H., and Axford, W. I. (1982). In 'Comets' (Ed. L. L. Wilkening), p. 588 (Univ. of Arizona Press: Tucson).
- Ip, W. H., Fink, U., and Johnson, J. R. (1985). *Astrophys. J.* **293**, 609.
- Janardhan, P., Alurkar, S. K., Bobra, A. D., and Slee, O. B., (1991). *Aust. J. Phys.* **44**, 565.
- Jockers, K. (1981). *Icarus* **47**, 397.
- Jockers, K. (1985). *Astron. Astrophys. Suppl. Ser.* **62**, 791.
- Little L. T. (1976). *Methods Exp. Phys.* **12c**, 118.
- Miller, F. D. (1970). *Icarus* **37**, 443.
- Ness, N. F., and Donn, B. D. (1965). *Mem. Soc. R. Liege Ser.* **5**, 12, 141.
- Readhead, A. C. S., and Hewish, A. (1974). *Mem. R. Astron. Soc.* **78**, 1.
- Readhead, A. C. S., Kemp, M. C., and Hewish, A. (1978). *Mon. Not. R. Astron. Soc.* **185**, 207.
- Saito, T., Saito, K., Aoki, T., and Yumoto, K. (1987). *Astron. Astrophys.* **18**, 201.
- Salpeter, E. E. (1967). *Astrophys. J.* **147**, 433.
- Scherb, F., Magee-Sauer, K., Roesler, F. L., and Harlander, J. (1990). *Icarus* **86**, 172.
- Schmidt, H. U., and Wegmann, R. (1982). In 'Comets' (Ed. L. L. Wilkening), p. 538 (Univ. of Arizona Press: Tucson).
- Schmidt-Voigt, M. (1989). *Astron. Astrophys.* **210**, 433.
- Slee, O. B., Bobra, A. D., Waldron, D., and Lim, J. (1990). *Aust. J. Phys.* **43**, 801.
- Slee, O. B., McConnell, D., Lim, J., and Bobra, A. D. (1987). *Nature* **325**, 699.